Muscle-Specific IRS-1 Ser→Ala Transgenic Mice Are Protected From Fat-Induced Insulin Resistance in Skeletal Muscle

Katsutaro Morino,[1,2] Susanne Neschen,[1,2] Stefan Bilz,[2] Saki Sono,[2] Dimitrios Tsirigotis,[2,3] Richard M. Reznick,[2,3] Irene Moore,[1] Yoshio Nagai,[1] Varman Samuel,[2] David Sebastian,[2] Morris White,[4] William Philbrick,[2] and Gerald I. Shulman[1,2,3]

OBJECTIVE—Insulin resistance in skeletal muscle plays a critical role in the pathogenesis of type 2 diabetes, yet the cellular mechanisms responsible for insulin resistance are poorly understood. In this study, we examine the role of serine phosphorylation of insulin receptor substrate (IRS)-1 in mediating fat-induced insulin resistance in skeletal muscle in vivo.

RESEARCH DESIGN AND METHODS—To directly assess the role of serine phosphorylation in mediating fat-induced insulin resistance in skeletal muscle, we generated muscle-specific IRS-1 Ser^{302}, Ser^{307}, and Ser^{612} mutated to alanine (Tg IRS-1 Ser→Ala) and IRS-1 wild-type (Tg IRS-1 WT) transgenic mice and examined insulin signaling and insulin action in skeletal muscle in vivo.

RESULTS—Tg IRS-1 Ser→Ala mice were protected from fat-induced insulin resistance, as reflected by lower plasma glucose concentrations during a glucose tolerance test and increased insulin-stimulated muscle glucose uptake during a hyperinsulinemic-euglycemic clamp. In contrast, Tg IRS-1 WT mice exhibited no improvement in glucose tolerance after high-fat feeding. Furthermore, Tg IRS-1 Ser→Ala mice displayed a significant increase in insulin-stimulated IRS-1–associated phosphatidylinositol 3-kinase activity and Akt phosphorylation in skeletal muscle in vivo compared with WT control littermates.

CONCLUSIONS—These data demonstrate that serine phosphorylation of IRS-1 plays an important role in mediating fat-induced insulin resistance in skeletal muscle in vivo. ***Diabetes*** **57:2644–2651, 2008**

Insulin resistance in skeletal muscle plays a major role in the pathogenesis of type 2 diabetes, yet the cellular mechanisms responsible for insulin resistance in skeletal muscle are poorly understood (1). Reduced insulin-stimulated glucose transport activity exists with reduced insulin receptor substrate (IRS)-1–associated phosphatidylinositol 3-kinase (PI3-kinase) activity in patients with type 2 diabetes and the offspring of type 2 diabetic parents (2–5). Increased serine phosphorylation of IRS-1 has been suggested to be responsible for this phenomenon (6), and, consistent with this hypothesis, recent studies have demonstrated hyperserine phosphorylation of IRS-1 on Ser^{302}, Ser^{307}, Ser^{612}, and Ser^{636} in several insulin-resistant rodent models (7–10), as well as in lean insulin-resistant offspring of type 2 diabetic parents (11). Circulating factors that are increased in obese and inflammatory states, such as tumor necrosis factor-α, activate Ser/Thr kinases (12,13). Also, recent studies (14–18) have demonstrated a strong relationship between intramyocelullar lipid accumulation and insulin resistance in muscle independent of alterations in circulating adipocytokines. Intramyocellular fatty acid metabolites, such as diacylglycerol, have been postulated to activate a serine kinase cascade leading to increased serine phosphorylation of IRS-1. Furthermore, high-fat diet–induced insulin resistance has been abrogated in rodent models in which certain Ser/Thr kinases (c-Jun N-terminal kinase, inhibitor of nuclear factor κB kinase β subunit, S6 kinase-1, and protein kinase C-θ) were either knocked down or pharmacologically inhibited (8,9,19–21). However, it remains unknown whether increased IRS-1 serine phosphorylation plays a causative role in the pathogenesis of fat-induced insulin resistance in skeletal muscle or whether it is merely an associated phenomenon. To address this question, we generated IRS-1 Ser^{302}, Ser^{307}, and Ser^{612} to Ala mutant–overexpression (Tg IRS-1 Ser→Ala) mice using a muscle-specific myosin light-chain-2 promoter and assessed insulin responsiveness in vivo by intraperitoneal glucose tolerance tests and hyperinsulinemic-euglycemic clamp studies.

RESEARCH DESIGN AND METHODS

Animals and dietary treatment. Tg IRS-1 Ser→Ala mutants were generated by microinjection of mutated IRS-1 (Ser^{302}, Ser^{307}, and Ser^{612}) complementary DNA constructs ligated to the myosin light-chain-2 promoter directly into fertilized oocytes, as described previously (22). Mice were backcrossed with C57BL/6J mice until the F_2-F_3 generation and male animals were selected for experiments in this study. All control mice (wild type [WT]) were littermates of the transgenic mice. From 25 positive founders, three lines were selected based on their protein expression of IRS-1 (approximately two times). These three lines showed similar phenotype when analyzed by intraperitoneal glucose tolerance tests (IPGTTs). To reduce the possibility of the mixed background attenuating the phenotype, we backcrossed one line for six generations but observed no metabolic phenotype differences between F_2 and F_6 backcross populations. Transgenic mice overexpressing WT murine IRS-1 (Tg IRS-1 WT) were generated by the same approach using exactly the same expression vector except for the mutated serine residues. Two lines were selected based on their protein expression of IRS-1 (approximately two times more IRS-1 protein in Tg IRS-1 WT). Mice were singly housed under standard vivarium conditions. At the age of 7–8 weeks, mice were started on a high-fat,

From the [1]Howard Hughes Medical Institute, Yale University School of Medicine, New Haven, Connecticut; the [2]Department of Internal Medicine, Yale University School of Medicine, New Haven, Connecticut; the [3]Department of Cellular and Molecular Physiology, Yale University School of Medicine, New Haven, Connecticut; and the [4]Howard Hughes Medical Institute, Children's Hospital Boston, Boston, Massachusetts.
Corresponding author: Gerald I. Shulman, gerald.shulman@yale.edu.
Received 6 April 2006 and accepted 3 July 2008.
Published ahead of print at http://diabetes.diabetesjournals.org on 15 July 2008. DOI: 10.2337/db06-0454.
K.M. and S.N. contributed equally to this article.

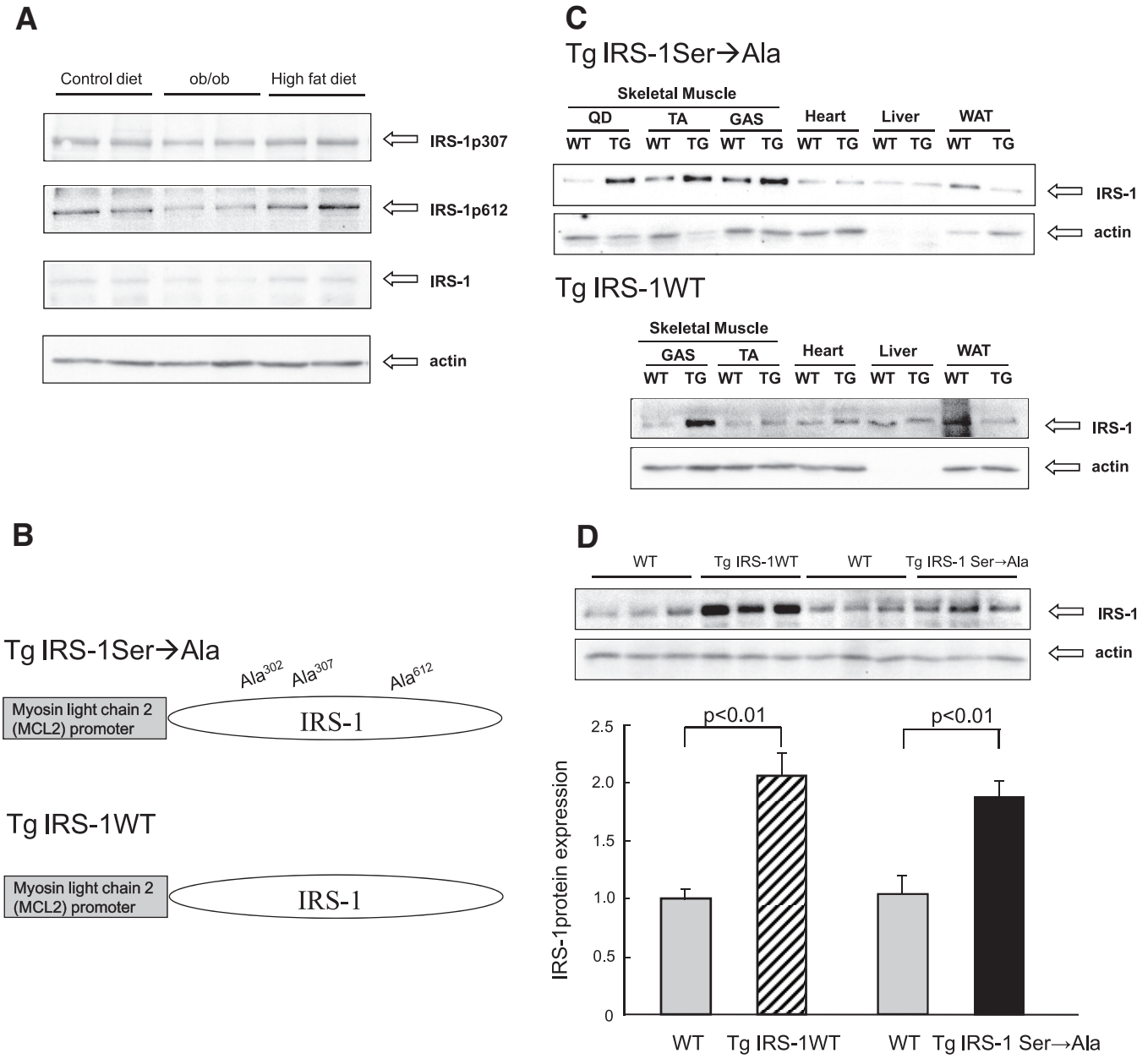

FIG. 1. Generation of Tg IRS-1 Ser→Ala mice. *A*: Serine phosphorylation of IRS-1 protein in skeletal muscle. Serine phosphorylation of IRS-1 and protein expression of IRS-1 were analyzed by Western blotting. All mice were killed at age 16 weeks. The high-fat diet group was fed for 8 weeks. *B*: Vector construct of the mutated IRS-1 gene (Ser^{302}, Ser^{307}, and Ser^{612} to Ala mutant) for Tg IRS-1 Ser→Ala and WT IRS-1 gene for Tg IRS-1 WT. *C*: Comparison of IRS-1 expression in different insulin-targeting tissues. Protein expression of total IRS-1 and actin were analyzed by Western blotting. *D*: Comparison of IRS-1 expression between Tg IRS-1 Ser→Ala and Tg IRS-1 WT mice. Each graph was expressed as fold difference to their littermates. GAS, *Musculus gastrocnemius*; QD, *Musclus quadriceps*; TA, *Musculus tibialis anterior*; WAT, white adipose tissue.

safflower oil–based diet (27% safflower oil and 59% fat-derived calories, 5.18 kcal/g) and maintained for 8 weeks. The safflower oil diet (no. 112245; Dyets, Bethlehem, PA) was supplemented with minerals and vitamins (no. 210025 and 310025). Food was exchanged every third day, and individual food consumption rates, body weight gain, and body composition using in vivo nuclear magnetic resonance spectroscopy (Minispec MQ10 analyzer; Bruker Optics, Billerica, MA) were measured at baseline and weekly throughout dietary intervention. After 4 weeks, high-fat diet feeding and IPGTT experiments (1 g glucose/kg body wt) were carried out. To examine Tg IRS-1 Ser→Ala in a different model, we also generated Tg IRS-1 Ser→Ala transgenic mice on *ob/ob* background according to a previous report (9). Briefly, we backcrossed Tg IRS-1 Ser→Ala with ob/$^{+}$ and mated Tg IRS-1 Ser→Ala/ob/$^{+}$ to generate Tg IRS-1 Ser→Ala/*ob/ob* and nontransgenic *ob/ob* (WT/*ob/ob*) mice.

For insulin-signaling experiments, mice received a single intraperitoneal injection of 0.6 units/kg insulin and tissues and plasma were harvested 15 min later. All experiments were performed in 16-h food-deprived mice. After an additional 4 weeks of high-fat diet treatment, hyperinsulinemic-euglycemic clamp experiments were performed. One week before clamp experiment, permanent catheters were inserted into the left jugular vein under deep anesthesia (intraperitoneal injection of ketamine/xylazine: 80/10 mg/kg body wt) and mice were allowed to regain preoperative weight for 5–7 days. All procedures were approved by the Yale University Animal Care and Use Committee.

Euglycemic-hyperinsulinemic glucose clamp experiments. Conscious mice were placed in restraining tubes and their tails were secured with tape. In vivo experiments lasted for 240 min and consisted of a 120-min basal period directly followed by a 120-min euglycemic-hyperinsulinemic clamp. Initiating the basal period, a prime-continuous [3-^{3}H]glucose infusion (10 μCi bolus, 0.1 μCi/min) was started and continued throughout the whole experiment, allowing the estimation of postabsorptive basal versus insulin-stimulated glucose turnover. At $t = 0$ min of the clamp, a primed-continuous insulin infusion (2.5 mU · kg^{-1} · min^{-1} Novolin; Novo Nordisc Pharmaceuticals, Princeton, NJ) was started, raising insulin levels within a physiologic range. Euglycemia was maintained by a variable glucose (D-20) infusion. Steady-

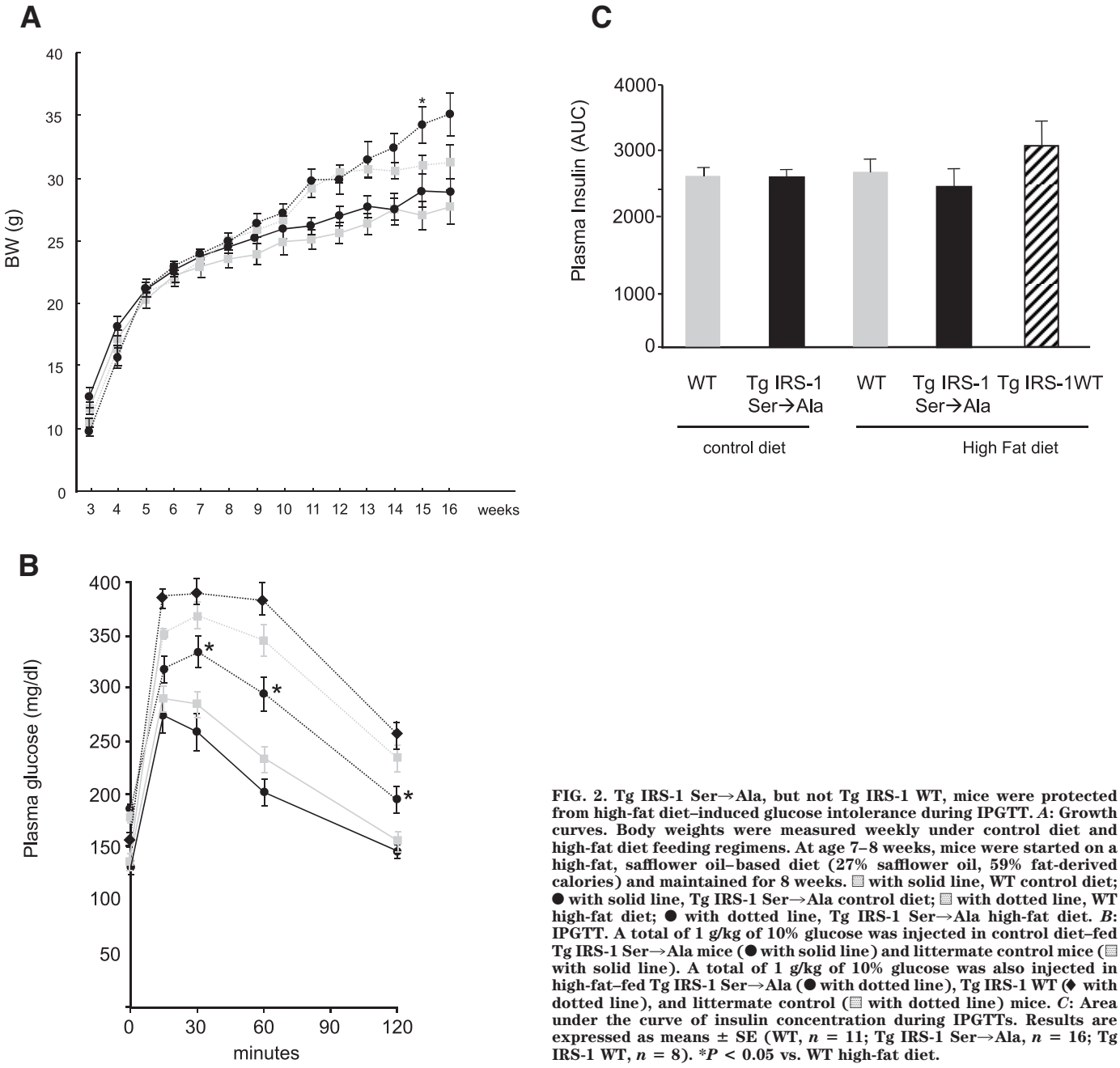

FIG. 2. Tg IRS-1 Ser→Ala, but not Tg IRS-1 WT, mice were protected from high-fat diet–induced glucose intolerance during IPGTT. *A*: Growth curves. Body weights were measured weekly under control diet and high-fat diet feeding regimens. At age 7–8 weeks, mice were started on a high-fat, safflower oil–based diet (27% safflower oil, 59% fat-derived calories) and maintained for 8 weeks. ▨ with solid line, WT control diet; ● with solid line, Tg IRS-1 Ser→Ala control diet; ▨ with dotted line, WT high-fat diet; ● with dotted line, Tg IRS-1 Ser→Ala high-fat diet. *B*: IPGTT. A total of 1 g/kg of 10% glucose was injected in control diet–fed Tg IRS-1 Ser→Ala mice (● with solid line) and littermate control mice (▨ with solid line). A total of 1 g/kg of 10% glucose was also injected in high-fat–fed Tg IRS-1 Ser→Ala (● with dotted line), Tg IRS-1 WT (♦ with dotted line), and littermate control (▨ with dotted line) mice. *C*: Area under the curve of insulin concentration during IPGTTs. Results are expressed as means ± SE (WT, n = 11; Tg IRS-1 Ser→Ala, n = 16; Tg IRS-1 WT, n = 8). *P < 0.05 vs. WT high-fat diet.

state conditions for plasma glucose concentration (121 ± 7 in Tg IRS-1 Ser→Ala vs. 131 ± 6 mg/dl in WT) and specific activities were achieved within 70 min, and a single 2-deoxy-D-[1-^{14}C]glucose (2-[^{14}C]DG) injection was administered at 75 min. To determine plasma [3-^{3}H]glucose and $^{3}H_2O$ and 2-[^{14}C]DG concentrations, blood samples were collected at 80, 85, 90, 100, 110, and 120 min of the clamp and, for measurement of basal [3-^{3}H]glucose concentrations, in the final 10 min of the basal period. A plasma sample for determination of basal insulin levels was obtained during the final 10 min of the basal period and for steady-state insulin levels (47 ± 5 in Tg IRS-1 Ser→Ala vs. 44 ± 5μU/ml in WT) at 120 min of the clamp. Infusions were performed using microdialysis pumps (CMA/Microdialysis, North Chelmsford, MA), and radioisotopes were purchased from Perkin Elmer Life Sciences (Boston, MA) and American Radiolabeled Chemicals (St. Louis, MO). At the end of the experiment, animals were anesthetized with intravenous ketamine/xylazine (80/10 mg/kg body wt), and epididymal white adipose tissue and M. gastrocnemius, including M. soleus, M. quadriceps, and liver, were collected, freeze-clamped, and stored at −80°C until further analysis.

Calculations. Steady-state period (when the rate of glucose appearance [R_a] equals the rate of glucose disappearance [R_d]) was defined as the final 20–30 min of the glucose clamp. The R_a was calculated as the ratio of [3-^{3}H]glucose infusion rate (dpm/min) and plasma [3-^{3}H]glucose–specific activity (dpm · min^{-1} · μmol^{-1}) during steady state. Hepatic [3-^{3}H]glucose production was determined by subtracting the steady-state glucose infusion rate from the R_a/R_d. Whole-body glycolysis was determined by linear regression from the increase of plasma $^{3}H_2O$ from 80 to 120 min (measured at 80, 85, 90, 100, 110, and 120 min). 2-[^{14}C]DG uptake in skeletal muscle was calculated from plasma 2-[^{14}C]DG area under the curve at 80, 85, 90, 100, 110, to 120 min and tissue 2-[^{14}C]DG-6-phosphate content using ion-exchange columns (Poly-Prep no. 731-6211; Bio-Rad, Hercules, CA) as previously described (4,23,24).

Assays from plasma. Glucose concentrations were determined with a glucose analyzer (Beckman, Fullerton, CA), and triacylglycerol and nonesterified fatty acid levels with a Kobas Mira Analyzer (Roche Diagnostics). Plasma insulin was measured via radioimmunoassay. Plasma [3-^{3}H]glucose, 2-[^{14}C]DG, and $^{3}H_2O$ radioactivity were determined from deproteinized plasma samples (somogyi filtrates) before and after $^{3}H_2O$ was completely evaporated from the supernatant. ^{3}H and ^{14}C radioactivity were assessed by use of a liquid scintillation counter (Ultima Gold; Packard Instrument, Meriden, CT).

Intramuscular triacylglycerol content. The extraction procedure for tissue triacylglycerol was adapted from methods described previously (25,26). Triacylglycerol content of each sample was measured in duplicate after evaporation of the organic solvent using an enzymatic method (Sigma Diagnostics, St. Louis, MO).

TABLE 1
Plasma metabolites and hormones in Tg IRS-1 Ser→Ala, Tg IRS-1 WT, and littermate control mice fed a safflower oil diet or a control diet for 4 weeks

	Control diet		High-fat diet		
	WT	Tg IRS-1 Ser→Ala	WT	Tg IRS-1 Ser→Ala	Tg IRS-1 WT
n	5–9	10–12	8–12	8–12	6
Glucose (mg/dl)	165 ± 7	143 ± 12	129 ± 11*	112 ± 17	122 ± 31
Insulin (μU/ml)	19.7 ± 3	21.0 ± 1.4	21.3 ± 1.5	16.5 ± 1.8*†	22.0 ± 1.8
Cholesterol (mg/dl)	88 ± 5.1	77 ± 3.5	82 ± 7	92 ± 6	74 ± 7
Triacylglycerol (mg/dl)	70 ± 11	89 ± 11	56 ± 3	57 ± 2	61 ± 5
Nonesterified fatty acids (mEq/l)	0.63 ± 0.04	0.61 ± 0.04	0.33 ± 0.04*	0.32 ± 0.05*	0.36 ± 0.05*
Intramuscular triacylglycerol content (μmol/g tissue)	1.50 ± 0.40	ND	2.39 ± 0.34*	3.11 ± 0.52*	ND

Data are means ± SE. *$P < 0.05$ vs. WT control diet. †$P < 0.05$ vs. WT high-fat diet.

Insulin signaling. To assess insulin-signaling molecules, Tg IRS-1 Ser→Ala, Tg IRS-1 WT, and WT mice were treated with 4 weeks of high-fat diet and gastrocnemius muscle was harvested 15 min after intraperitoneal insulin injection (0.6 units/kg). Western blot and immunoprecipitation were performed as described previously (27). Briefly, samples were homogenized in a buffer containing 50 mmol/l Hepes (pH 7.4), 150 mmol/l NaCl, 1 mmol/l EDTA, 1% Triton X-100, 2 mmol/l sodium vanadate, 100 mmol/l NaF, 20 mmol/l sodium pyrophosphate, 20 mg/ml of aprotinin, and 1 mmol/l phenylmethylsulphonyl fluoride. One milligram of lysate was subjected to immunoprecipitation and incubated with 4 mg of anti–IRS-1 or –IRS-2 antibody (Upstate Biotechnology) for 2 h at 4°C and then with protein A/G agarose (Santa Cruz) overnight. The beads were washed three times before immunoblot analysis. Samples were denatured with Laemmli sample buffer for 5 min at 95°C, and the supernatant was separated using 10% SDS gel (Bio-Rad Laboratories) and electrotransferred onto polyvinylidene fluoride membranes (Amersham Pharmacia Biotech). Samples were probed with anti-phosphotyrosine (4G10-HRP; Upstate Biotechnology) and anti-p85 antibody (Upstate Biotechnology). IRS-1– and IRS-2–associated PI3-kinase assays were performed in 4 mg muscle protein extracts according to methods previously described (28). Western blotting was performed as described previously (27). Forty micrograms of homogenized samples were blotted on polyvinylidene fluoride membranes. The membrane was probed with antibodies against phospho-Akt (Ser^{473}) (1:1,000; Cell Signaling), IRS-1 (1:1,000; Upstate Biotechnology), IRS-1pSer307 (1:1,000; Cell Signaling), and IRS-1pSer612 (1:1,000; Cell Signaling) overnight at 4°C. Antibodies against IRS-1pSer307 and IRS-1pSer612 were diluted in the enhancer solution (Can Get Signal Solution; Toyobo, Osaka, Japan). Equal protein loading was confirmed by reblotting of the membranes with a goat polyclonal antibody to pan-actin (1:1,000; Santa Cruz Biotechnology) or anti-Akt antibody (1:1,000; Cell Signaling). Images were analyzed and quantified with Quantity One (Bio-Rad Laboratories).

Statistical analysis. All data are expressed as means ± SE. Two-tailed Student's *t* tests were performed on data at a minimum $P < 0.05$ threshold.

RESULTS

High-fat diet increased serine phosphorylation of IRS-1. To evaluate previous reports regarding increased serine phosphorylation on IRS-1 in skeletal muscle, we tested Ser^{307} and Ser^{612} residues using high-fat–fed mice and *ob/ob* mice. We found slight increases on Ser^{307} and Ser^{612} but decreased total IRS-1 protein in *ob/ob* mice (Fig. 1*A*).

Generation of IRS-1 Ser→Ala mutant transgenic and Tg IRS-1 WT mice. To investigate the role of serine phosphorylation on IRS-1 in mediating fat-induced insulin resistance, we generated skeletal muscle–specific transgenic mice with triple mutations in Ser^{302}, Ser^{307}, and Ser^{612} to Ala using the 1.2-kb enhancer/promoter region of the myosin light-chain-2 gene (Fig. 1*B*). Total IRS-1 protein expression levels were analyzed in multiple insulin target organs. We observed ~100% overexpression of IRS-1 exclusively in skeletal muscles in transgenic mice compared with their WT littermates (Fig. 1*C* and *D*). To address whether the phenotype of Tg IRS-1 Ser→Ala protection against fat-induced insulin resistance depended on the Ser→Ala mutation of IRS-1, and not on the overexpression of IRS-1 per se, we also generated mice overexpressing WT IRS-1 (Tg IRS-1 WT) as an alternative control (Fig. 1*B*). Using the same approach, we created a line of Tg IRS-1 WT mice that expressed IRS-1 WT protein in skeletal muscle approximately twofold more than the WT littermates (Fig. 1*C* and *D*).

Metabolic phenotype in standard diet–fed Tg IRS-1 Ser→Ala and their littermates. Growth curves of Tg IRS-1 Ser→Ala and WT mice were comparable between standard diet–fed groups (Fig. 2*A*). Tg IRS-1 Ser→Ala mice displayed no differences in any basal parameters (Table 1) and had similar plasma glucose responses following an intraperitoneal glucose challenge when fed a control standard diet (Fig. 2*B*). The body composition of these mice, analyzed by ^{1}H-nuclear magnetic resonance spectroscopy, were similar in both genotypes (77.0 ± 0.6% of muscle and 8.5 ± 0.6% of fat in WT vs. 75.8 ± 1.0% of muscle and 9.4 ± 1.3% of fat in Tg IRS-1 Ser→Ala; $P = 0.28$ and $P = 0.50$, respectively). Overexpression of mutated IRS-1, but not WT IRS-1, rescued high-fat diet–induced glucose intolerance. To determine whether the Ser→Ala mutation of IRS-1 would protect mice from fat-induced insulin resistance in skeletal muscle, we fed WT, Tg IRS-1 Ser→Ala, and Tg IRS-1 WT mice a high-fat diet containing 27% safflower oil for 4 weeks. Tg IRS-1 Ser→Ala and WT mice increased their whole-body fat content in a comparable fashion (data not shown) but gained slightly more body weight than WT mice (Fig. 2*A*). Tg IRS-1 WT gained similar body weight after 4 weeks of high-fat regimen (30 ± 0.5 g at age 12 weeks). There were no differences in fasting plasma glucose, cholesterol, triacylglycerol, and nonesterified fatty acid concentrations among the three groups, yet plasma insulin concentrations were 23% lower in the Tg IRS-1 Ser→Ala mutant than the WT mice (Table 1). Intramuscular triacylglycerol content after high-fat feeding showed no difference between the two genotypes (Table 1). When IPGTT experiments were performed after 4 weeks of high-fat feeding, Tg IRS-1 Ser→Ala mice displayed a markedly improved glucose tolerance (Fig. 2*B*), despite no differences in plasma insulin concentrations (Fig. 2*C*), compared with both WT and Tg IRS-1 WT mice fed a similar high-fat diet.

Overexpression of mutated IRS-1 rescued high-fat diet induced insulin resistance in skeletal muscle. To determine which tissue was responsible for the enhanced

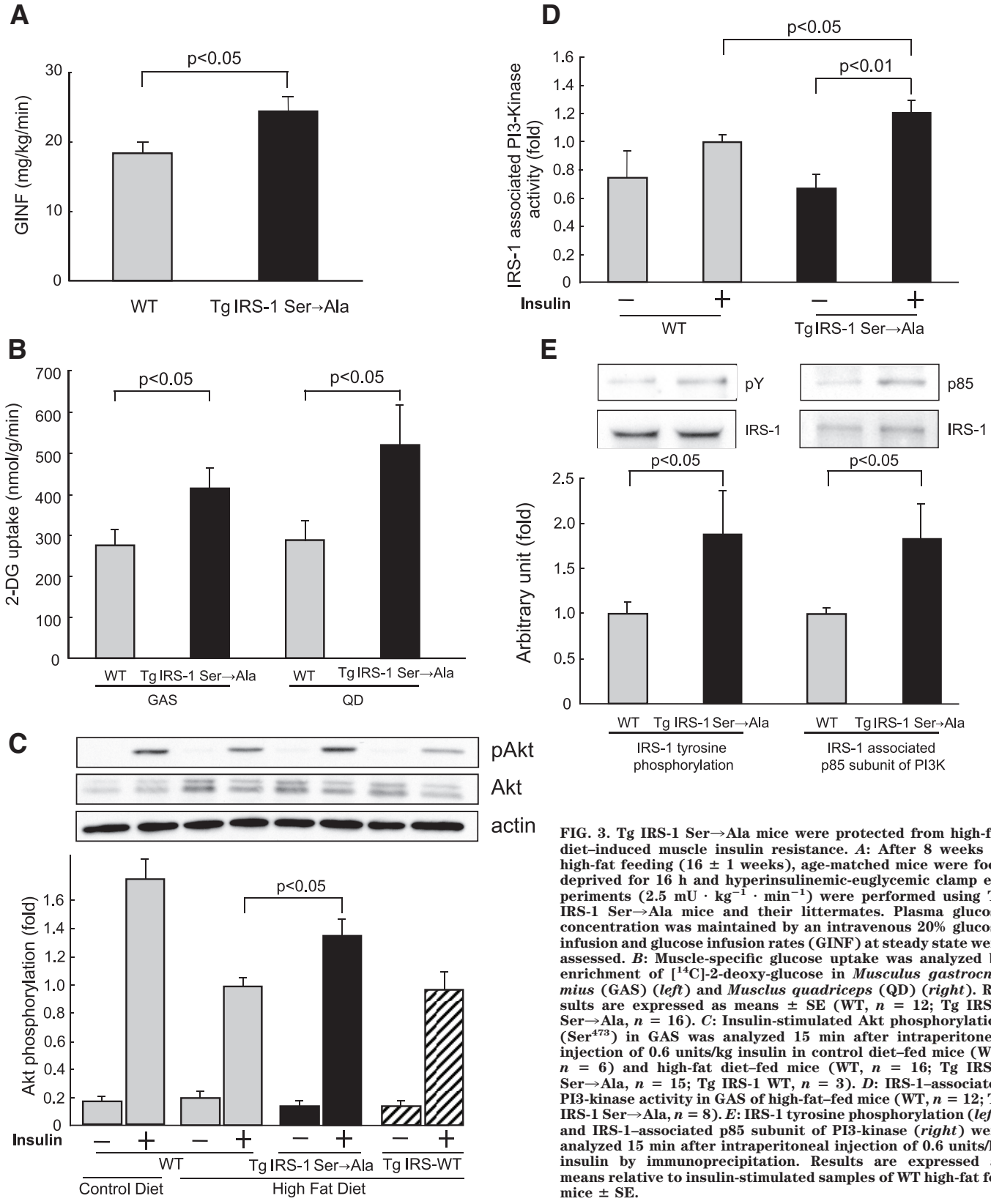

FIG. 3. Tg IRS-1 Ser→Ala mice were protected from high-fat diet–induced muscle insulin resistance. *A*: After 8 weeks of high-fat feeding (16 ± 1 weeks), age-matched mice were food deprived for 16 h and hyperinsulinemic-euglycemic clamp experiments (2.5 mU · kg^{-1} · min^{-1}) were performed using Tg IRS-1 Ser→Ala mice and their littermates. Plasma glucose concentration was maintained by an intravenous 20% glucose infusion and glucose infusion rates (GINF) at steady state were assessed. *B*: Muscle-specific glucose uptake was analyzed by enrichment of [^{14}C]-2-deoxy-glucose in *Musculus gastrocnemius* (GAS) (*left*) and *Musclus quadriceps* (QD) (*right*). Results are expressed as means ± SE (WT, *n* = 12; Tg IRS-1 Ser→Ala, *n* = 16). *C*: Insulin-stimulated Akt phosphorylation (Ser^{473}) in GAS was analyzed 15 min after intraperitoneal injection of 0.6 units/kg insulin in control diet–fed mice (WT, *n* = 6) and high-fat diet–fed mice (WT, *n* = 16; Tg IRS-1 Ser→Ala, *n* = 15; Tg IRS-1 WT, *n* = 3). *D*: IRS-1–associated PI3-kinase activity in GAS of high-fat–fed mice (WT, *n* = 12; Tg IRS-1 Ser→Ala, *n* = 8). *E*: IRS-1 tyrosine phosphorylation (*left*) and IRS-1–associated p85 subunit of PI3-kinase (*right*) were analyzed 15 min after intraperitoneal injection of 0.6 units/kg insulin by immunoprecipitation. Results are expressed as means relative to insulin-stimulated samples of WT high-fat fed mice ± SE.

glucose tolerance in the Tg IRS-1 Ser→Ala mice, we performed hyperinsulinemic-euglycemic clamp experiments in age-matched WT and Tg IRS-1Ser→Ala mice after 8 weeks of high-fat diet treatment. Tg IRS-1 Ser→Ala mice manifested greater insulin sensitivity, as reflected by a 34% increased in glucose infusion rate required to maintain euglycemia during the clamp (Fig. 3*A*). Further analysis of plasma and skeletal muscle tracer data revealed a 50% increase in insulin-stimulated 2-deoxy-D-[1-14C]glucose uptake in both the gastrocnemius muscles (274.2 ± 39.9 nmol · g^{-1} · min^{-1} vs. 414.9 ± 46.3 nmol · g^{-1} · min^{-1}; $P < 0.05$) and the quadriceps muscles (287.6 ±

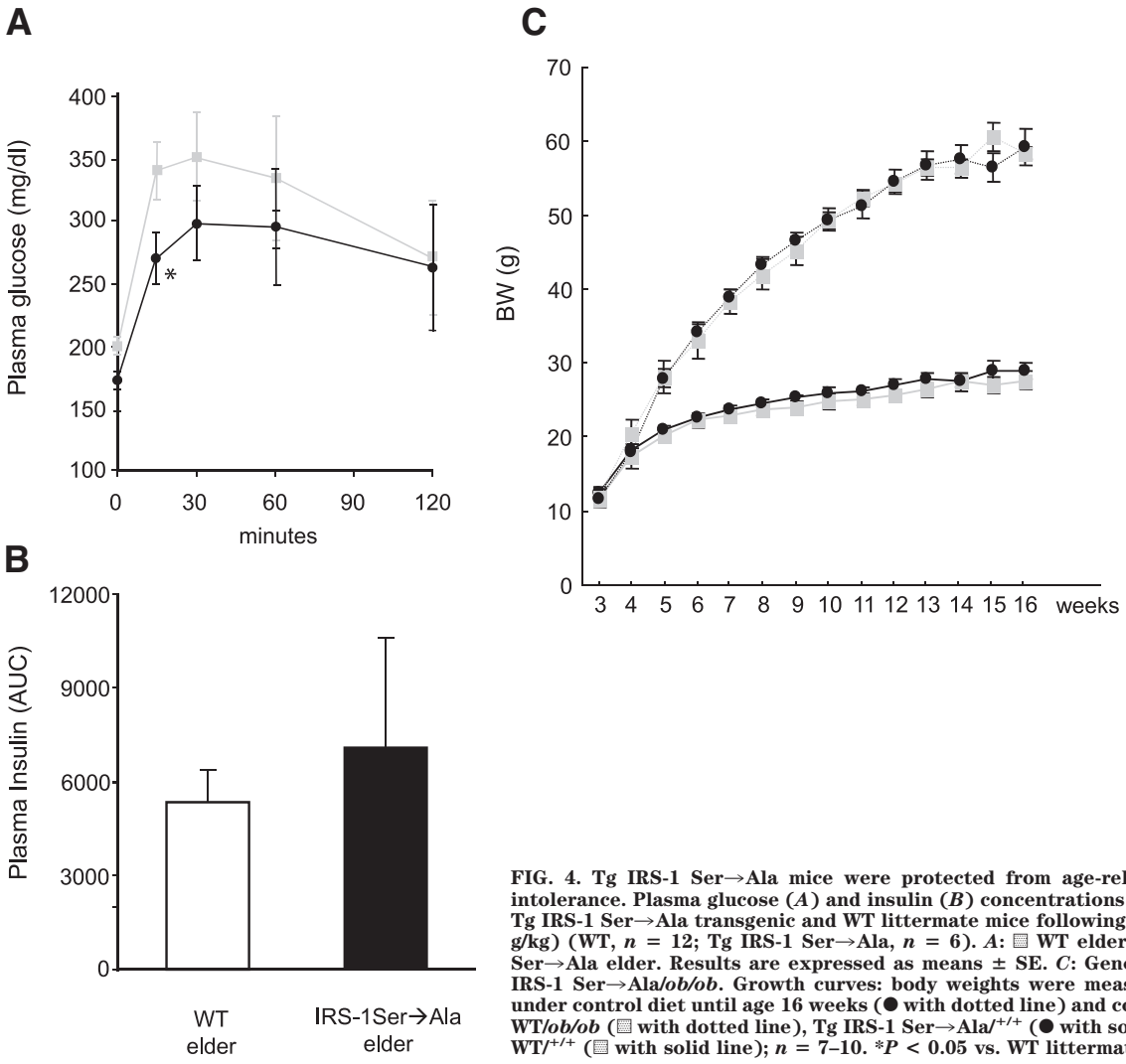

FIG. 4. Tg IRS-1 Ser→Ala mice were protected from age-related glucose intolerance. Plasma glucose (*A*) and insulin (*B*) concentrations in 1-year-old Tg IRS-1 Ser→Ala transgenic and WT littermate mice following an IPGTT (1 g/kg) (WT, $n = 12$; Tg IRS-1 Ser→Ala, $n = 6$). *A*: ▨ WT elder; ♦, Tg IRS-1 Ser→Ala elder. Results are expressed as means ± SE. *C*: Generation of Tg IRS-1 Ser→Ala/*ob/ob*. Growth curves: body weights were measured weekly under control diet until age 16 weeks (● with dotted line) and compared with WT/*ob/ob* (▨ with dotted line), Tg IRS-1 Ser→Ala/$^{+/+}$ (● with solid line), and WT/$^{+/+}$ (▨ with solid line); $n = 7$–10. *$P < 0.05$ vs. WT littermate mice.

48.3 nmol · g^{-1} · min^{-1} vs. 0.518.9 ± 98.1 nmol · g^{-1} · min^{-1}; $P < 0.05$) (Fig. 3*B*). In contrast, there were no differences in insulin-mediated suppression of hepatic glucose production between the Tg IRS-1 Ser→Ala and the WT mice (basal 16.6 ± 1.0 vs. 17.6 ± 1.2 mg · kg^{-1} · min^{-1}, insulin-stimulated 5.0 ± 3.7 vs. 0.1 ± 2.8 mg · kg^{-1} · min^{-1}; $P = 0.27$).

Ser→Ala mutation on IRS-1, but not overexpression of IRS-1, improved insulin signaling. To further analyze the mechanism for the improved insulin-stimulated muscle glucose uptake in the Tg IRS-1 Ser→Ala mice, we assessed insulin signaling in vivo after 4 weeks of high-fat diet treatment. High-fat feeding reduced insulin-stimulated Akt phosphorylation in gastrocnemius muscle after 15 min of intraperitoneal insulin injection in WT mice; however, we observed a 32% increase in Akt phosphorylation in Tg IRS-1 Ser→Ala mice compared with WT littermates (Fig. 3*C*). We also analyzed insulin-induced Akt phosphorylation in Tg IRS-1 WT, but we did not observe significant improvement in Tg IRS-1 WT (Fig. 3*C*). We also detected a 20% increase in IRS-1–associated PI3-kinase activity (Fig. 3*D*) of Tg IRS-1 Ser→Ala compared with WT mice in absence of changes in IRS-2–associated PI3-kinase activity (data not shown). Furthermore, tyrosine phosphorylation of IRS-1 was increased by 88% in Tg IRS-1 Ser→Ala mice compared with WT littermates (Fig. 3*E*, *left*). IRS-1–associated p85 subunit of PI3-kinase was also 83% higher in Tg IRS-1 Ser→Ala mice (Fig. 3*E*, *right*).

Overexpression of mutated IRS-1 improved glucose metabolism in old mice and Tg IRS-1 Ser→Ala mice bred onto an *ob/ob* background. To analyze the effect of overexpression of mutated IRS-1 in different insulin resistance models, we tested these mice at age 1 year with an IPGTT. Tg IRS-1 Ser→Ala mice showed better glucose tolerance compared with their littermates at age 1 year, although they had similar insulin concentration during IPGTT (Fig. 4*A* and *B*) and similar body weight (Tg IRS-1 Ser→Ala 48.1 ± 0.7 vs. WT 48.5 ± 0.3). In addition, we also examined the effect of backcrossing the Tg IRS-1 Ser→Ala mice onto an *ob/ob* background and found lower fasting plasma glucose concentrations in the Tg IRS-1 Ser→Ala/*ob/ob* compared with the WT/*ob/ob* mice (306 ± 23 mg/dl vs. 218 ± 9 mg/dl; $P = 0.005$) at age 4 weeks. Although growth curves of IRS-1 Ser→Ala/*ob/ob* and WT/*ob/ob* were comparable (Fig. 4*C*), fasting glucose of IRS-1 Ser→Ala/*ob/ob* tended to be lower throughout their life until age 16 weeks than WT/*ob/ob* mice (data not shown).

DISCUSSION

Our study demonstrates that serine phosphorylation on IRS-1 is a key molecular event in the pathogenesis of

fat-induced insulin resistance in vivo. Although IRS-1 has >70 potential serine/threonine phosphorylation sites, we observed that mutating the serines at Ser^{302}, Ser^{307}, and Ser^{612} to alanines partially, but significantly, protected the mice against fat-induced insulin resistance in skeletal muscle. Previous in vitro studies speculated four possible mechanisms by which serine phosphorylation of IRS-1 can inhibit the insulin-signaling pathway. First, it has been reported that serine phosphorylation on Ser^{302}, Ser^{307}, and Ser^{318} inhibits the association between the insulin receptor and IRS-1 because Ser^{302} and Ser^{307} exist near the phosphotyrosine binding domain (155–259), where the insulin receptor binds to IRS-1 (29–31). Second, serine phosphorylation has been shown to interfere with the tyrosine phosphorylation of IRS-1 (32). Third, phosphorylation on Ser^{612}, Ser^{632}, Ser^{662}, and Ser^{731} has been demonstrated to inhibit the association between IRS-1 and the p85 subunit of PI3-kinase (31,33). Finally, serine phosphorylation or IRS-1 on certain sites such as Ser^{307} has been shown to promote protein degradation through the ubiquitin-proteosome pathway and/or the suppressor of cytokine-signaling pathway (34–36). The data in the present study support the hypothesis that in vivo IRS-1 serine phosphorylation intereferes with IRS-1 tyrosine phosphorylation by the first three mechanisms, since we found increased insulin-stimulated IRS-1 tyrosine phosphorylation in the Tg IRS-1 Ser→Ala mice (Fig. 3*D*), suggesting at least one of three serine residues regulate interaction between insulin receptor and IRS-1 and/or tyrosine phosphorylation. Furthermore, Tg IRS-1 Ser→Ala mice also showed an increased association between IRS-1 and the p85 subunit of PI3-kinase, which reflects increased interaction between IRS-1 and PI 3-kinase likely due to the Ser^{612}→Ala^{612} mutation (33,37). On the other hand, our data suggest that IRS-1 serine phosphorylation does not lead to increased IRS-1 degradation by activation of the ubiquitin-proteosome or suppressor of cytokine-signaling pathway, since IRS-1 protein expression was unchanged after 8 weeks of high-fat diet treatment (Fig. 1*A*). These data are also consistent with recent studies in humans demonstrating unaltered IRS-1 expression in the muscle of young lean insulin-resistant offspring of parents with type 2 diabetes (11). In contrast to these results, we did observed decreased IRS-1 protein expression in *ob/ob* mice compared with WT mice (Fig. 1*A*), suggesting that increased IRS-1 degradation may occur in the *ob/ob* phenotype, which is consistent with a previous study (38).

To address whether the IRS-1 Ser→Ala mutation protection from fat-induced insulin resistance depended on the Ser→Ala mutation of IRS-1 and not on the overexpression of IRS-1 per se, we also generated mice with a similar twofold overexpression of WT IRS-1 (Tg IRS-1 WT) in skeletal muscle as an alternative control. In contrast to the Tg IRS-1 Ser→Ala mice, Tg IRS-1 WT mice were not protected from high-fat–induced glucose intolerance during IPGTT. Furthermore, in contrast to Tg IRS-1 Ser→Ala mice, Tg IRS-1 WT mice were also not protected from fat-induced defects in insulin stimulation of Akt phosphorylation in skeletal muscle. These findings are consistent with a recent study demonstrating that whole-body IRS-1 overexpressing mice were also not protected from insulin resistance (39). Taken together, these data support the hypothesis that the protection from fat-induced insulin resistance observed in the Tg IRS-1 Ser→Ala mice is due to the Ser→Ala IRS mutation and not due to IRS-1 WT overexpression.

In summary, our study supports the hypothesis that high-fat diet–induced insulin resistance in skeletal muscle is mediated at least in part through increased serine phosphorylation of IRS-1. This event may be a potential pharmacological target in the treatment of insulin resistance associated with obesity and type 2 diabetes.

ACKNOWLEDGMENTS

This work was supported by grants from the U.S. Public Health Service (R01 DK-40936, U24 DK-76169, and P30 DK-45735), the Uehara Memorial Foundation (to K.M.), and a Distinguished Clinical Scientist Award from the American Diabetes Association (to G.I.S.). G.I.G. is an investigator of the Howard Hughes Medical Institute.

We thank Aida Grossmann, Rebecca Pongratz, Yanna Kosover, Jörg Rossbacher, Mario Kahn, Gary Cline, Patricia Donovan, and Tom Nuzzo for excellent technical assistance.

REFERENCES

1. Shulman GI, Rothman DL, Jue T, Stein P, DeFronzo RA, Shulman RG: Quantitation of muscle glycogen-synthesis in normal subjects and subjects with non-insulin-dependent diabetes by C-13 nuclear magnetic-resonance spectroscopy. *N Engl J Med* 322:223–228, 1990
2. Shulman GI: Cellular mechanisms of insulin resistance. *J Clin Invest* 106:171–176, 2000
3. Dresner A, Laurent D, Marcucci M, Griffin ME, Dufour S, Cline GW, Slezak LA, Andersen DK, Hundal RS, Rothman DL, Petersen KF, Shulman GI: Effects of free fatty acids on glucose transport and IRS-1-associated phosphatidylinositol 3-kinase activity. *J Clin Invest* 103:253–259, 1999
4. Yu CL, Chen Y, Cline GW, Zhang DY, Zong HH, Wang YL, Bergeron R, Kim JK, Cushman SW, Cooney GJ, Atcheson B, White MF, Kraegen EW, Shulman GI: Mechanism by which fatty acids inhibit insulin activation of insulin receptor substrate-1 (IRS-1)-associated phosphatidylinositol 3-kinase activity in muscle. *J Biol Chem* 277:50230–50236, 2002
5. Griffin ME, Marcucci MJ, Cline GW, Bell K, Barucci N, Lee D, Goodyear LJ, Kraegen EW, White MF, Shulman GI: Free fatty acid–induced insulin resistance is associated with activation of protein kinase C θ and alterations in the insulin signaling cascade. *Diabetes* 48:1270–1274, 1999
6. Tanasijevic MJ, Myers MG, Thoma RS, Crimmins DL, White MF, Sacks DB: Phosphorylation of the insulin-receptor substrate IRS-1 by casein kinase-Ii. *J Biol Chem* 268:18157–18166, 1993
7. Werner ED, Lee JS, Hansen L, Yuan MS, Shoelson SE: Insulin resistance due to phosphorylation of insulin receptor substrate-1 at Serine 302. *J Biol Chem* 279:35298–35305, 2004
8. Um SH, Frigerio F, Watanabe M, Picard F, Joaquin M, Sticker M, Fumagalli S, Allegrini PR, Kozma SC, Auwerx J, Thomas G: Absence of S6K1 protects against age- and diet-induced obesity while enhancing insulin sensitivity. *Nature* 431:200–205, 2004
9. Hirosumi J, Tuncman G, Chang LF, Gorgun CZ, Uysal KT, Maeda K, Karin M, Hotamisligil GS: A central role for JNK in obesity and insulin resistance. *Nature* 420:333–336, 2002
10. Rui LY, Aguirre V, Kim JK, Shulman GI, Lee A, Corbould A, Dunaif A, White MF: Insulin/IGF-1 and TNF-alpha stimulate phosphorylation of IRS-1 at inhibitory Ser(307) via distinct pathways. *J Clin Invest* 107:181–189, 2001
11. Morino K, Petersen KF, Dufour S, Befroy D, Frattini J, Shatzkes N, Neschen S, White MF, Bilz S, Sono S, Pypaert M, Shulman GI: Reduced mitochondrial density and increased IRS-1 serine phosphorylation in muscle of insulin-resistant offspring of type 2 diabetic parents. *J Clin Invest* 115:3587–3593, 2005
12. Hotamisligil GS, Peraldi P, Budavari A, Ellis R, White MF, Spiegelman BM: IRS-1-mediated inhibition of insulin receptor tyrosine kinase activity in TNF-alpha- and obesity-induced insulin resistance. *Science* 271:665–668, 1996
13. Aytug S, Reich D, Sapiro LE, Bernstein D, Begum N: Impaired IRS-1/PI3-kinase signaling in patients with HCV: a mechanism for increased prevalence of type 2 diabetes. *Hepatology* 38:1384–1392, 2003
14. Perseghin G, Scifo P, De Cobelli F, Pagliato E, Battezzati A, Arcelloni C, Vanzulli A, Testolin G, Pozza G, Del Maschio A, Luzi L: Intramyocellular triglyceride content is a determinant of in vivo insulin resistance in humans: a H-1-C-13 nuclear magnetic resonance spectroscopy assessment in offspring of type 2 diabetic parents. *Diabetes* 48:1600–1606, 1999
15. Krssak M, Petersen KF, Dresner A, DiPietro L, Vogel SM, Rothman DL,

Shulman GI, Roden M: Intramyocellular lipid concentrations are correlated with insulin sensitivity in humans: a H-1 NMR spectroscopy study. *Diabetologia* 42:113–116, 1999
16. Petersen KF, Befroy D, Dufour S, Dziura J, Ariyan C, Rothman DL, DiPietro L, Cline GW, Shulman GI: Mitochondrial dysfunction in the elderly: possible role in insulin resistance. *Science* 300:1140–1142, 2003
17. Petersen KF, Dufour S, Befroy D, Garcia R, Shulman GI: Impaired mitochondrial activity in the insulin-resistant offspring of patients with type 2 diabetes. *N Engl J Med* 350:664–671, 2004
18. Morino K, Petersen KF, Shulman GI: Molecular mechanisms of insulin resistance in humans and their potential links with mitochondrial dysfunction. *Diabetes* 55 (Suppl. 2):S9–S15, 2006
19. Yuan MS, Konstantopoulos N, Lee JS, Hansen L, Li ZW, Karin M, Shoelson SE: Reversal of obesity- and diet-induced insulin resistance with salicylates or targeted disruption of IKK beta. *Science* 293:1673–1677, 2001
20. Kim JK, Fillmore JJ, Sunshine MJ, Albrecht B, Higashimori T, Kim DW, Liu ZX, Soos TJ, Cline GW, O'Brien WR, Littman DR, Shulman GI: PKC-theta knockout mice are protected from fat-induced insulin resistance. *J Clin Invest* 114:823–827, 2004
21. Furukawa N, Ongusaha P, Jahng WJ, Araki K, Choi CS, Kim HJ, Lee YH, Kaibuchi K, Kahn BB, Masuzaki H, Kim JK, Lee SW, Kim YB: Role of Rho-kinase in regulation of insulin action and glucose homeostasis. *Cell Metabolism* 2:119–129, 2005
22. Dunbar ME, Dann P, Brown CW, Van Houton J, Dreyer B, Philbrick WP, Wysolmerski JJ: Temporally regulated overexpression of parathyroid hormone-related protein in the mammary gland reveals distinct fetal and pubertal phenotypes. *J Endocrinol* 171:403–416, 2001
23. Ohshima K, Shargill NS, Chan TM, Bray GA: Adrenalectomy reverses insulin resistance in muscle from obese (Ob/Ob) mice. *Am J Physiol* 246:E193–E197, 1984
24. Ren JM, Marshall BA, Mueckler MM, Mccaleb M, Amatruda JM, Shulman GI: Overexpression of Glut4 protein in muscle increases basal and insulin-stimulated whole-body glucose disposal in conscious mice. *J Clin Invest* 95:429–432, 1995
25. Frayn KN, Maycock PF: Skeletal-muscle triacylglycerol in the rat: methods for sampling and measurement, and studies of biological variability. *J Lipid Res* 21:139–144, 1980
26. Neschen S, Morino K, Hammond LE, Zhang DY, Liu ZX, Romanelli AJ, Cline GW, Pongratz RL, Zhang XM, Choi CS, Coleman RA, Shulman GI: Prevention of hepatic steatosis and hepatic insulin resistance in mitochondrial acyl-CoA: glycerol-sn-3-phosphate acyltransferase 1 knockout mice. *Cell Metabolism* 2:55–65, 2005
27. Samuel VT, Liu ZX, Qu XQ, Elder BD, Bilz S, Befroy D, Romanelli AJ, Shulman GI: Mechanism of hepatic insulin resistance in non-alcoholic fatty liver disease. *J Biol Chem* 279:32345–32353, 2004
28. Bruning JC, Winnay J, Cheatham B, Kahn CR: Differential signaling by insulin receptor substrate 1 (IRS-1) and IRS-2 in IRS-1-deficient cells. *Mol Cell Biol* 17:1513–1521, 1997
29. Paz K, Hemi R, LeRoith D, Karasik A, Elhanany E, Kanety H, Zick Y: Elevated serine/threonine phosphorylation of IRS-1 and IRS-2 inhibits their binding to the juxtamembrane region of the insulin receptor and impairs their ability to undergo insulin-induced tyrosine phosphorylation. *J Biol Chem* 272:29911–29918, 1997
30. Aguirre V, Werner ED, Giraud J, Lee YH, Shoelson SE, White MF: Phosphorylation of Ser(307) in insulin receptor substrate-1 blocks interactions with the insulin receptor and inhibits insulin action. *J Biol Chem* 277:1531–1537, 2002
31. Moeschel K, Beck A, Weigert C, Lammers R, Kalbacher H, Voelter W, Schleicher ED, Haring HU, Lehmann R: Protein kinase C-zeta-induced phosphorylation of Ser(318) in insulin receptor substrate-1 (IRS-1) attenuates the interaction with the insulin receptor and the tyrosine phosphorylation of IRS-1. *J Biol Chem* 279:25157–25163, 2004
32. Li JP, Defea K, Roth RA: Modulation of insulin receptor substrate-1 tyrosine phosphorylation by an Akt/phosphatidylinositol 3-kinase pathway. *J Biol Chem* 274:9351–9356, 1999
33. Mothe I, VanObberghen E: Phosphorylation of insulin receptor substrate-1 on multiple serine residues, 612, 632, 662, and 731, modulates insulin action. *J Biol Chem* 271:11222–11227, 1996
34. Egawa K, Nakashima N, Sharma PM, Maegawa H, Nagai Y, Kashiwagi A, Kikkawa R, Olefsky JM: Persistent activation of phosphatidylinositol 3-kinase causes insulin resistance due to accelerated insulin-induced insulin receptor substrate-1 degradation in 3T3-L1 adipocytes. *Endocrinology* 141:1930–1935, 2000
35. Pederson TM, Kramer DL, Rondinone CM: Serine/threonine phosphorylation of IRS-1 triggers its degradation: possible regulation by tyrosine phosphorylation. *Diabetes* 50:24–31, 2001
36. Rui LY, Yuan MS, Frantz D, Shoelson S, White MF: SOCS-1 and SOCS-3 block insulin signaling by ubiquitin-mediated degradation of IRS1 and IRS2. *J Biol Chem* 277:42394–42398, 2002
37. Ravichandran LV, Esposito DL, Chen J, Quon MJ: Protein kinase C-zeta phosphorylates insulin receptor substrate-1 and impairs its ability to activate phosphatidylinositol 3-kinase in response to insulin. *J Biol Chem* 276:3543–3549, 2001
38. Kerouz NJ, Hörsch D, Pons S, Kahn CR: Differential regulation of insulin receptor substrates-1 and -2 (IRS-1 and IRS-2) and phosphatidylinositol 3-kinase isoforms in liver and muscle of the obese diabetic (ob/ob) mouse. *J Clin Invest* 100:3164–3172, 1997
39. Murata Y, Tsuruzoe K, Kawashima J, Furukawa N, Kondo T, Motoshima H, Igata M, Taketa K, Sasaki K, Kishikawa H, Kahn CR, Toyonaga T, Araki E: IRS-1 transgenic mice show increased epididymal fat mass and insulin resistance. *Biochem Biophys Res Commun* 364:301–307, 2007